Boussac, A., Zimmermann, J. L., Rutherford, A. W., & Lavergne, J. (1991) *Nature 347*, 303-306.
Chylla, R., Garab, G., & Whithmarsh, J. (1987) in *Progress in Photosynthesis Research* (Biggins, J., Ed.) Vol. 2, pp 237-240, Martinus Nijhoff, Dordrecht.
Dekker, J. P., Van Gorkom, H. J., Wensink, J., & Ouwehand, L. (1984) *Biochim. Biophys. Acta 767*, 1-9.
Förster, V., & Junge, W. (1985) *Photochem. Photobiol. 41*, 183-190.
Fowler, C. F. (1977a) *Biochim. Biophys. Acta 462*, 414-421.
Fowler, C. F. (1977b) *Biochim. Biophys. Acta 459*, 351-363.
Fowler, C. F., & Kok, B. (1976) *Biochim. Biophys. Acta 423*, 510-523.
Ghanotakis, D. F., & Babcock, G. T. (1983) *FEBS Lett. 153*, 231-234.
Graan, T., & Ort, D. R. (1987) in *Progress in Photosynthesis Research* (Biggins, J., Ed.) Vol. 2, pp 241-244, Martinus Nijhoff, Dordrecht.
Jahns, P., Lavergne, J., Rappaport, F., & Junge, W. (1991) *Biochim. Biophys. Acta 1057*, 313-319.
Joliot, P., & Kok, B. (1975) in *Bioenergetics of Photosynthesis* (Govindjee, Ed.) pp 387-412, Academic Press.
Joliot, P., & Joliot, A. (1984) *Biochim. Biophys. Acta 765*, 210-218.
Joliot, P., Béal, D., & Frilley, B. (1980) *J. Chim. Phys. 77*, 209-216.
Lavergne, J. (1987) *Biochim. Biophys. Acta 894*, 91-107.
Lavergne, J. (1991) *Biochim. Biophys. Acta* (in press).
Lavergne, J., & Rappaport, F. (1990) in *Current Research in Photosynthesis* (Baltscheffsky, M., Ed.) Vol. 1, pp 873-876, Kluwer Academic Publishers, Dordrecht.
Lavorel, J. (1978) *J. Theor. Biol. 57*, 171-185.
Lübbers, K., & Junge, W. (1990) in *Current Research in Photosynthesis* (Baltscheffsky, M., Ed.) Vol. 1, pp 877-880, Kluwer Academic Publishers, Dordrecht.
Maroti, P., & Wraight, C. A. (1988) *Biochim. Biophys. Acta 934*, 329-347.
McPherson, P. H., Okamura, M. Y., & Feher, G. (1988) *Biochim. Biophys. Acta 934*, 348-368.
Meyer, B., Schlodder, E., Dekker, J. P., & Witt, H. T. (1989) *Biochim. Biophys. Acta 974*, 36-43.
Petrouleas, V., & Diner, B. (1986) *Biochim. Biophys. Acta 849*, 264-275.
Polle, A., & Junge, W. (1986) *Biochim. Biophys. Acta 848*, 257-264.
Rutherford, A. W. (1989) *Trends Biochem. Sci. 14*, 227-232.
Saphon, S., & Crofts, A. R. (1977) *Z. Naturforsch. 32C*, 617-626.
Saygin, O., & Witt, H. T. (1985) *FEBS Lett. 178*, 224-226.
Vass, I., & Styring, S. (1991) *Biochemistry 30*, 830-839.
Velthuys, B. R. (1988) *Biochim. Biophys. Acta 933*, 249-257.
Wacker, U., Haag, E., & Renger, G. (1990) in *Current Research in Photosynthesis* (Baltscheffsky, M., Ed.) Vol. 1, pp 869-872, Kluwer Academic Publishers, Dordrecht.

Differences in Thermal Stability between Reduced and Oxidized Cytochrome b_{562} from *Escherichia coli*†

Mark T. Fisher*
Laboratory of Biochemistry, National Heart, Lung and Blood Institute, National Institutes of Health, Bethesda, Maryland 20892

Received May 21, 1991; Revised Manuscript Received July 29, 1991

ABSTRACT: The thermal stabilities of ferri- and ferrocytochrome b_{562} were examined. Thermally induced spectral changes, monitored by absorption and second-derivative spectroscopies, followed the dissociation of the heme moiety and the increased solvation of tyrosine residue(s) located in close proximity to the heme binding site. All observed thermal transitions were independent of the rate of temperature increase (0.5–2 °C/min), and the denatured protein exhibited partial to near-complete reversibility upon return to ambient temperature. The extent of renaturation of cytochrome b_{562} is dependent on the amount of time the unfolded conformer is exposed to temperatures above the transition temperature, T_m. All thermally induced spectra changes fit a simple two-state model, and the thermal transition was assumed to be reversible. The thermal transition for ferrocytochrome b_{562} yielded T_m and van't Hoff enthalpy (ΔH_{vH}) values of 81.0 °C and 137 kcal/mol, respectively. In contrast, T_m and ΔH_{vH} values obtained for the ferricytochrome were 66.7 °C and 110 kcal/mol, respectively. The estimated increase in the stabilization free energy at the T_m of ferricytochrome b_{562} following the one-electron reduction to the ferrous form, where $\Delta\Delta G = \Delta T_m \Delta S_m$ [ΔS_m = 324 cal/(K·mol), ΔT_m = 14.3 °C] [Becktel, W. J., & Schellman, J. A. (1987) *Biopolymers 26*, 1859-1877], is 4.6 kcal/mol.

Cytochrome b_{562} from *Escherichia coli* is a small (M_r 12000) water-soluble heme protein and is localized in the periplasmic space. This cytochrome contains an N-terminal leader sequence which is subsequently cleaved during or after transport through the inner periplasmic membrane (Nikkila, 1987). Although its functional role in *E. coli* is unknown, cytochrome b_{562} from *Acinetobacter calcoaceticus* has been proposed to function as an electron-transfer shuttle between the quinoprotein glucose dehydrogenase (+50 mV), localized in the periplasm, and ubiquinone (Doktor et al., 1988).

The structure of the *E. coli* cytochrome has been defined by X-ray crystallography to a resolution of 2.5 Å (Mathews et al., 1979). The protein folds in an antiparallel α-helical

† Preliminary experiments, performed in Dr. S. G. Sligar's laboratory, were supported by NIH Grants GM 33775 and GM 31756.
* Address correspondence to this author at NHLBI/NIH, Building 3, Room 207, Bethesda, MD 20892.

motif consisting of four helices. The heme, protoporphyrin IX, is noncovalently bound and is coordinated to the protein through His-106 and Met-7. This cytochrome has a redox potential of +180 mV at pH 7.0 (Moore et al., 1985). One face of the heme moiety is exposed to solvent with the propionic side chains of the heme forming part of a localized distribution of negative charge surrounded by four acidic side chains of the N-terminal helix and the C-terminal carboxyl group of Arg-106. This negative charge distribution near the heme edge presumably aids in electrostatic steering and determines the biological specificity of interaction of this cytochrome with its physiological electron donor(s) or acceptor(s) (Matthew et al., 1983).

The existence of conformational differences between redox states of electron-transfer proteins can directly affect the activation energy for the electron-transfer reaction by contributing to the nuclear reorganizational energy (Marcus & Sutin, 1985). The reorganizational energy is a major determinate of the electron-transfer rate in biological systems. If redox-linked conformational changes are slower than the electron-transfer rate, there is the possibility that the electron-transfer step is "gated" (Hoffman & Ratner, 1987). Such "gated" electron-transfer events have been proposed to occur in the cytochrome c/b_2 complex (McLendon et al., 1987), ruthenated cytochrome c (Bechtold et al., 1986), and cytochrome oxidase (Gray & Malmström, 1989).

One common type of global conformational change which appears to accompany a change in redox state for electron-transfer proteins is an alteration in the flexibility of the protein. For example, under conditions of low ionic strength, the protein structure of ferricytochrome c is characterized by a larger apparent compressibility and increased radius of gyration compared with the reduced form of the protein (Eden et al., 1982; Kharakoz & Mkhitaryan, 1986; Trewhella et al., 1988). The increased flexibility of ferricytochrome c over the reduced form is also inferred from increases in hydrogen exchange rates following oxidation of the protein at moderate ionic strengths (Ulmer & Kagi, 1968; Wand et al., 1986). The redox-dependent flexibility differences may be a result of changes in the formal charge on the iron (Eden et al., 1982). In redox proteins, at least one oxidation state carries a net charge inside the protein matrix. The creation and stabilization of a charged moiety in a protein interior could be accomplished by subtle changes in surface charge through redox shifts in pK_a's or the creation of a neutralizing charge near the redox center or both. Differences in elution profiles of ferri- vs ferrocytochrome from cation-exchange columns suggest that changes in the surface charge may accompany the redox reaction of this protein (Margoliash, 1954).

Significant structure differences between redox states of electron-transfer proteins can be compared by measuring redox-dependent shifts in the enthalpy, entropy, and transition temperature (T_m) for a thermally induced unfolding reaction. Cytochrome b_{562} is a potential model system which can be used to further characterize important structural differences that occur in redox proteins following an electron-transfer event. Results presented herein describe the thermal unfolding differences between ferri- and ferrocytochrome b_{562}.

Materials and Methods

Protein Solutions and Chemicals. Cytochrome b_{562} was purified by using an overproducing strain of *E. coli* (TB-1) carried in a pUC19 plasmid (Nikkila, 1987). The protein was purified according to published procedures (Itagaki & Hager, 1966) to a ratio of A_{418}/A_{280} of 5.6. Potassium phosphate buffer (0.1 M, pH 7.0, 25 °C) was used throughout the thermal transition experiments. Protein concentrations were determined from the molar extinction coefficients of 0.180 μM^{-1} cm^{-1} at 426 nm or 0.0316 μM^{-1} cm^{-1} at 562 nm for the reduced conformer and 0.117 μM^{-1} cm^{-1} at 418 nm or 0.0106 μM^{-1} cm^{-1} at 532 nm for the oxidized from (Itagati & Hager, 1966). Protein concentrations of 2.5–3.5 μM were used for the thermal denaturation studies unless specified. Acridine was purchased from Aldrich Chemical Co. EDTA was purchased from Sigma. Ultrapure guanidine hydrochloride (Gdn-HCl)[1] was purchased from Schwarz/Mann Biotech.

All absorption difference and second-derivative spectra were obtained by using a Hewlett-Packard 8450A rapid-scan diode array spectrophotometer. The sample and reference cells were maintained at temperature with a Hewlett-Packard 89100A temperature control station with attached Hewlett-Parkard 89101A Pelter junction cell holders. The solution temperature was monitored by using a Hewlett-Packard 89102A temperature probe. Throughout temperature cycling, the solutions were stirred with the aid of small cuvette magnetic stir bars.

Thermal Analysis. The temperature-dependent spectral changes were recorded after the system reached equilibrium or as a function of time during a programmed temperature ramp. For the thermal equilibrium analysis, the temperature of the protein solution was increased in 2 °C increments followed by 5–10-min equilibration times to ensure that thermal equilibrium was reached. Adequate equilibration was confirmed throughout the thermal transition zone by monitoring the thermally induced changes in the Soret absorption at the temperature of measurement as a function of time. Equilibrium conditions were noted by the lack of significant spectral changes. At the temperature of measurement, an entire spectrum (220–800 nm) was recorded at 2 spectra per second for 60 s, and the resulting spectrum was the average of 120 measurements.

Another series of experiments examined the thermal transition profiles resulting from temperature-dependent spectral changes of the heme at a single wavelength as the rate of temperature increase was varied. This method was used to evaluate the dependence of the thermodynamic parameters, notably the van't Hoff enthalpy (ΔH_{vH}) and transition temperature (T_m), on the thermal scan rate. The thermal unfolding of the oxidized cytochrome was followed by monitoring the heme absorption differences ($A_{418} - A_{800}$ or $A_{532} - A_{800}$) as a function of time at a defined temperature increase rate (degrees centigrade per minute). The temperature-dependent absorption changes of the reduced protein were monitored by the absorption differences $A_{426} - A_{800}$ or $A_{562} - A_{800}$.

Second-Derivative Spectroscopy. Solvation changes for tyrosine residues were observed by second-derivative difference spectroscopy (Demchenko, 1986). Cytochrome b_{562} contains two tyrosine and two phenylalanine residues. The protein concentration of the cytochrome used for monitoring the temperature-dependent second-derivative UV absorption changes was 30 μM to enhance the signal/noise ratio. The initial (25 °C) second-derivative spectrum (255–300 nm) was stored and used as a base-line spectrum. Second-derivative spectra were recorded with increasing temperature after equilibration, and a temperature-dependent second-derivative absorption difference spectrum was obtained by subtracting the spectrum recorded at the temperature of measurement from the base-line spectrum.

Reduction of Ferricytochrome b_{562}. Ferrocytochrome b_{562} is oxidized in the presence of O_2 at a rate of 0.029 min^{-1} at

[1] Abbreviations: EDTA, ethylenediaminetetraacetic acid; Gdn-HCl, guanidine hydrochloride.

25 °C (Fisher, unpublished results). Therefore, all thermal transition experiments for the ferrous form of the protein were performed under anaerobic conditions by using the method outlined by Englander et al. (1987). Cytochrome b_{562} was photoreduced by illumination of the anaerobic solution with a fluorescent lamp in the presence of 1–2 mM EDTA and 0.5–1.6 μM acridine. The observed thermodynamic parameters did not depend on the concentration of dye or EDTA present in solution. The photoreduction system was perferred to that using dithionite because dithionite is unstable at the high temperatures required to perform these experiments. Reduction was monitored by the absorbance ratio 562 nm/600 nm. Complete reduction of the cytochrome (25 °C) was confirmed on separate samples by the lack of further spectral changes after addition of a small amount of dithionite.

Anaerobic solutions of cytochrome b_{562} were obtained as follows. The phosphate buffer was subjected to at least four cycles of vacuum degassing and argon purging in an anaerobic Thunberg cuvette (Precision NGS cells). The protein and components of the photoreduction system were added, and the solution was subjected to two more degassing/purge cycles. The cuvette was opened under a continuous flow of argon and layered with degassed/purged mineral oil to ensure against oxygen diffusion. The mineral oil layer also prevented evaporation of the sample during the thermal unfolding experiments and long-term incubations after temperature cycling. Long-term incubations at ambient temperatures were used to observed the slow regain of the cytochrome absorption. Under these conditions (25 °C), the reduced cytochrome (kept in the dark) exhibited no measurable oxidation by atmospheric oxygen for 2 days as reflected by the stable Soret absorption peaks. Difference spectra revealed that no oxidation occurred during or after the thermal transition. For both programmed temperature increases and thermal equilibration experiments, the temperature probe was inserted through the mineral oil layer to monitor the solution temperature. Again, no oxidation was observed at ambient temperature under these conditions.

Kinetics of Gdn-HCl-Induced Heme Dissociation. Gdn-HCl-induced time-dependent decreases in heme absorption were followed by monitoring the decrease in the Soret absorption at 418 and 426 nm for ferri- and ferrocytochrome b_{562}, respectively. Ferricytochrome b_{562} (3.8 μM final concentration) was rapidly mixed with the aid of a magnetic stir bar (dead time 5 s) with a buffer solution containing Gdn-HCl (4 M final concentration) at 25 °C. Single-wavelength measurements were obtained every second until the reaction was complete (i.e., no further changes in Soret absorbance). To monitor the Gdn-HCl-induced heme dissociation from ferrocytochrome b_{562}, an anaerobic solution containing approximately 7 μM cytochrome was reduced with dithionite (1 mM final concentration). An equal volume of an anaerobic buffer solution (also overlaid with mineral oil) containing 8 M Gdn-HCl and 1 mM dithionite was added to the cuvette through the mineral oil overlay with the aid of an air-tight Hamilton syringe and was mixed with a magnetic stir bar. The loss of heme absorption for ferrocytochrome b_{562} was considerably slower, and as a consequence, the kinetics were analyzed by using the Guggenhiem method. Briefly, after complete mixing, the entire spectrum was recorded every 0.5 h for 20 h. After 48 h, a second time-dependent kinetic analysis was obtained every 0.5 h for another 20 h. Second-derivative absorption changes were recorded at 426 nm to eliminate complications due to base-line drift and light scattering (Demchenko, 1984). As a control, an anaerobic buffer (no Gdn-HCl, 2 mM dithionite) was added to a duplicate solution

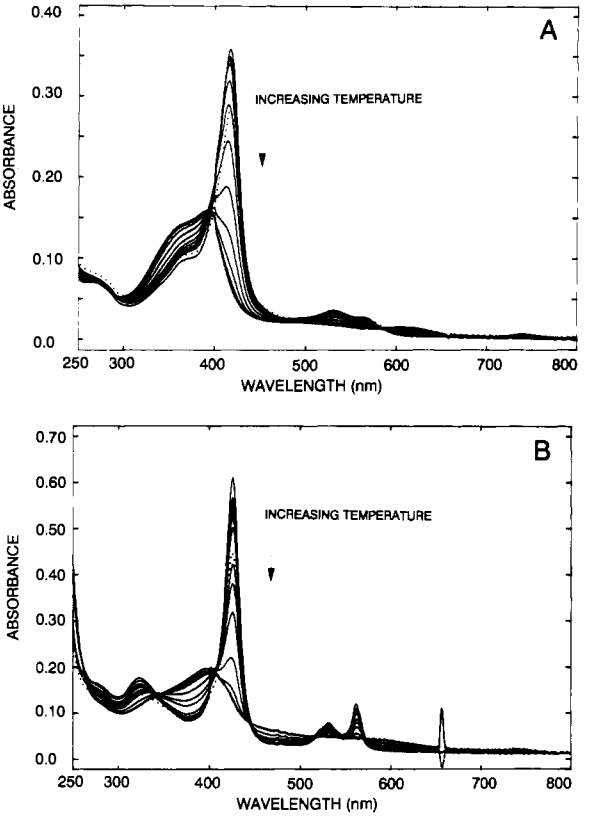

FIGURE 1: Representative thermally induced absorption spectra for (A) oxidized and (B) reduced cytochrome b_{562}. The concentration of oxidized and reduced cytochrome was 3.0 and 3.5 μM, respectively, in 100 mM potassium phosphate buffer at pH 7.0 (25 °C). Each temperature-dependent spectrum was recorded after a 5–10-min equilibration time through a temperature range of 25–80 and 90 °C for the oxidized and reduced conformers, respectively. The initial return spectra at 25 °C after thermal cycling are also shown (···).

of dithionite-reduced cytochrome b_{562}. No oxidation was observed in the control solution over the length of time used to monitor the heme dissociation (88 h). The kinetics of heme absorption changes due to the presence of 4 M Gdn-HCl were evaluated by using the Guggenheim method (Guggenheim, 1926):

$$\ln (A_t - A_{t+dt}) = -kt + \text{constant} \quad (1)$$

where A_t is the absorbance at time t and A_{t+dt} is the absorbance at time t + 48 h. A linear relationship between ln $(A_t - A_{t+dt})$ and t would indicate that the reaction follows a first-order process. The slope of this linear plot yields the rate, k.

Results

Thermal Stability of Ferri- and Ferrocytochrome b_{562}. Changes in the heme absorption spectra were obtained when ferri- and ferrocytochrome b_{562} were subjected to varying temperature (Figure 1). The existence of numerous isosbestic points for the oxidized and reduced cytochrome over the chosen wavelength range indicates that the observed temperature effects can be described as a simple two-state system.

The high-temperature heme absorption spectra of the oxidized and reduced forms exhibit considerable blue shifts and are broadened with absorption maxima at 391 and 387 nm, respectively. These high-temperature spectra are characteristic of free heme and suggest that the heme moiety has dissociated from the protein. The thermally induced spectral changes were reversible for both redox forms of the cytochrome. The extent of recovery of the original spectrum (at 25 °C) after thermal unfolding was dependent on the duration the unfolded conformer was exposed to temperatures above the transition

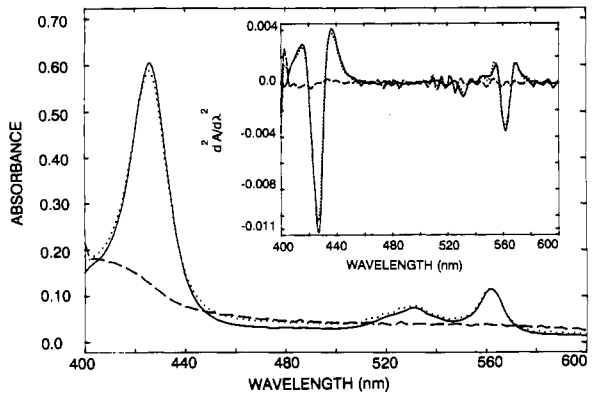

FIGURE 2: Thermal transition is reversible. Representative spectra for the reduced cytochrome b_{562} at 25 °C initial (—), 90 °C, 5-min equilibration (---), and 25 °C return spectra (···) after 1 h. Inset: Second-derivative spectra of the heme-dependent absorption changes were used to eliminate any contributions due to base-line shifts and light scattering. Comparison of the second-derivative amplitudes before and after a 90 °C temperature incubation indicates that 95% of the initial heme absorption is regained following a 1-h incubation at 25 °C.

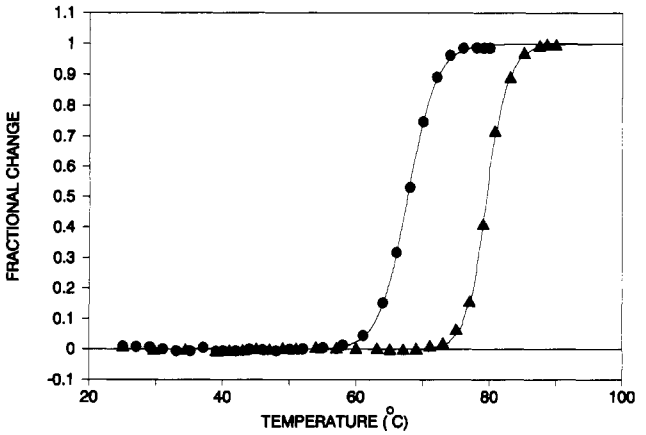

FIGURE 3: Base-line-corrected thermally induced fractional changes for oxidized (●) and reduced (▲) cytochrome b_{562} monitored at 418 and 426 nm, respectively. These data were fit by assuming a two-state unfolfing process. The calculated enthalpy changes (ΔH_{vH}) and transition temperatures (T_m) for the oxidized and reduced species shown above are 110 kcal/mol, 67.3 °C and 137 kcal/mol, 80.7 °C, respectively.

temperature. The existence of thermal reversibility was confirmed as follows: After a rapid increase in temperature (5 min) from 25 to 80 °C (oxidized) or 90 °C (reduced), the sample was allowed to equilibrate, and the solution temperature was rapidly returned to 25 °C. Under these conditions, 95% of the original reduced cytochrome absorption spectrum returned within 1 h (Figure 2). Under conditions where thermal equilibrium measurements were obtained (slow increases in temperature), the cytochrome absorption showed partial recovery to the original native spectrum. The absorption spectrum for both the reduced and the oxidized cytochrome slowly returned to the original spectrum during long-term incubations (16 h) at 25 °C.

The thermally induced heme spectral changes indicate that the cytochrome unfolds in a single cooperative transition. The pre- and postdenaturation base lines were determined by a linear least-squares analysis. The thermal unfolding equilibrium constant for N ⇌ D, $K_{eq}(T)$, was determined by the relationship:

$$K_{eq} = \frac{A_N(T) - A(T)}{A(T) - A_D(T)} \quad (2)$$

where $A(T)$ is the absorbance at temperature T and $A_N(T)$ and $A_D(T)$ are the absorbances at temperature T derived form the extrapolated base lines. The van't Hoff enthalpy (ΔH_{vH}), transition temperature (T_m), and A_{max} were obtained from the equations

$$K_{eq} = \exp[-\Delta H_{vH}(1/T - 1/T_m)/R] \quad (3)$$

$$\Delta A_{calcd} = \Delta A_{max} K_{eq}/(1 + K_{eq}) \quad (4)$$

The ΔA values (after subtraction of the extrapolated base lines) were fit with the corresponding ΔA_{calcd} values by adjustment of the above indicated parameters with a nonlinear least-squares program. A comparison of the two-state van't Hoff thermal transition profiles for ferri- and ferrocytochrome b_{562} indicates that the one-electron-reduced form of the cytochrome is more resistant to thermal denaturation than is the oxidized conformer (Figure 3). More significantly, reduction of cytochrome b_{562} is accompanied by a dramatic increase in the transition temperature (T_m, where $K_{eq} = 1$) of 14.3 °C and an increase in enthalpy by 27 kcal/mol (Table I).

The existence of additional species following thermally induced heme dissociation was indicated by the partial recovery

Table I: Experimental Thermodynamic Data for the Thermal Unfolding of Ferri- and Ferrocytochrome b_{562}[a]

cytochrome species	T_m (°C)	ΔH_{vH} (kcal/mol)	ΔS [cal/(K·mol)]
ferri			
heme absorption changes (7)	66.7 ± 0.5	110 ± 6	324 ± 17
second-derivative tyrosine solvation changes (3)	68.4 ± 3.1	125 ± 13	366 ± 44
ferro			
heme absorption changes (6)	81.0 ± 0.5	137 ± 10	380 ± 23

[a] Parenthetical values represent the number of experimental trials. All thermodynamic values are for T_m, where T_m(K) = T_m(°C) + 273.15. The enthalpy and T_m values are the best-fit values obtained from the simultaneous three-parameter, iterative, nonlinear fits to eq 3 and 4 of the data (ΔA vs T).

of the heme absorption spectrum at 25 °C (Figure 1). Sturtevant and co-workers have recently shown that DSC-measured thermal transitions for several proteins which irreversibly denature can be treated by the van't Hoff relationship, in spite of calorimetric irreversibility (Manly et al., 1985; Edge et al., 1985; Hu & Sturtevant, 1987). Under these conditions, the unfolding transition is represented by

$$N \underset{k_2}{\overset{k_1}{\rightleftharpoons}} D \overset{k_3}{\rightarrow} I$$

where N, D, and I represent native, denatured, and irreversibly denatured conformers, respectively. This model predicts that the van't Hoff enthalpy and T_m will be independent of the thermal scan rate if k_3 is small relative to the rate of thermal equilibrium (N ⇌ D). The effect of varying the rate of temperature increase on the derived ΔH_{vH} and T_m values for both redox species is summarized in Table II. The results indicate that the enthalpies and transition temperatures are very similar as the temperature ramp rate increases even though the extent of recovery decreases with decreasing temperature ramp rates in most instances. The invariant ΔH_{vH} and T_m values support the assumption that the temperature-dependent spectral changes can be fit to a true thermal equilibrium.

For both the oxidized and reduced conformers of cytochrome b_{562}, the extent of recovery slowly increased when the samples were heated, cooled, and allowed to stand for 16 h. The existence of a slow reversible step following thermally

Table II: Dependence of the Rate of Temperature Increase on the Thermodynamic Parameters ΔH_{vH} and T_m for Ferri- and Ferrocytochrome b_{562}

cytochrome species	ΔT_m (°C/min)	ΔH_{vH} (kcal/mol)	T_m (°C)	% initial return	% 16-h return[a]
ferri	2	110	66.3	75	85
	1	109	66.5	65	74
	0.5	107	66.5	59	68
	0.2	114	66.3	42	50
ferro	0.6	140	81.2	72	85
	0.3	135	81.7	69	77
	0.2	144	80.8	66	72

[a] All cytochrome solutions were layered with degassed and argon-purged mineral oil to prevent evaporation during temperature cycling and long-term incubations monitoring slow recovery of the initial cytochrome spectrum.

induced heme dissociation and protein unfolding suggests that the thermal unfolding transition for this cytochrome can be represented as

$$N \underset{}{\overset{\text{fast}}{\rightleftharpoons}} D \overset{\text{slow}}{\rightleftharpoons} D' \rightarrow I$$

where the $D \rightleftharpoons D'$ and $D' \rightarrow I$ reactions are slow in comparison to the kinetics of the $N \rightleftharpoons D$ equilibrium. Here, D' represents another reversible denatured for of the protein and is in slow equilibration with the initial D form. Characterization of D' and I species was not attempted. Alternatively, it is possible that the I species can also arise from the the first denatured D form and a different mechanism would have to be invoked.

Thermally Induced Second-Derivative Changes in the UV Region (250–300 nm). Cytochrome b_{562} has two phenylalanine and two tyrosine residues, and both are positioned near the heme group (Mathews et al., 1979). The thermally induced changes in tyrosine solvation for the oxidized conformer show a significant blue shift as indicated by the increased second-derivative absorbance contribution in the second-derivative difference spectra. This behavior is characteristic of increased solvation surrounding these residues (Figure 4A). Furthermore, the two-state van't Hoff thermal transition profiles for both the thermally induced heme absorbances and the second-derivative absorbance changes monitored by tyrosine-dependent changes at 287 nm are coincident (Figure 4B). This indicates that increased solvation of the heme binding region accompanies the loss of the heme group during thermal denaturation. In addition, a characteristic blue shift and loss of intensity were also observed for the second-derivative absorbance peaks in the wavelength region attributed to phenylalanine absorbance (240–270 nm) following thermal denaturation (Ichikawa & Terada, 1979). Although the absorbance due to phenylalanine is too low to obtain a meaningful thermal transition profile, the increase in solvation of these residues is also consistent with the temperature-induced heme release.

Kinetics of Gdn-HCl-Dependent Heme Dissociation. The stability differences between ferri- and ferrocytochrome b_{562} were probed by altering the heme binding equilibrium using Gdn-HCl as a perturbant. The dissociation of heme from the cytochrome was observed by monitoring decreases in the characteristic Soret absorbance at 418 nm ($\Delta A = A_{418} - A_{800}$) for the ferricytochrome and in the second-derivative absorbance ($\Delta A''$) at 426 nm ($\Delta A'' = A''_{426} - A''_{490}$) for the ferrocytochrome. The rate profiles of the Gdn-HCl-induced heme dissociation from the oxidized and reduced cytochromes fit first-order decay processes with calculated rates of 6.2×10^{-2} and 4.8×10^{-6} s^{-1} at 25 °C, respectively. Due to the extremely slow dissociation of reduced heme from the cytochrome under these conditions, the kinetic rate of this reaction was obtained by a Guggenheim analysis.

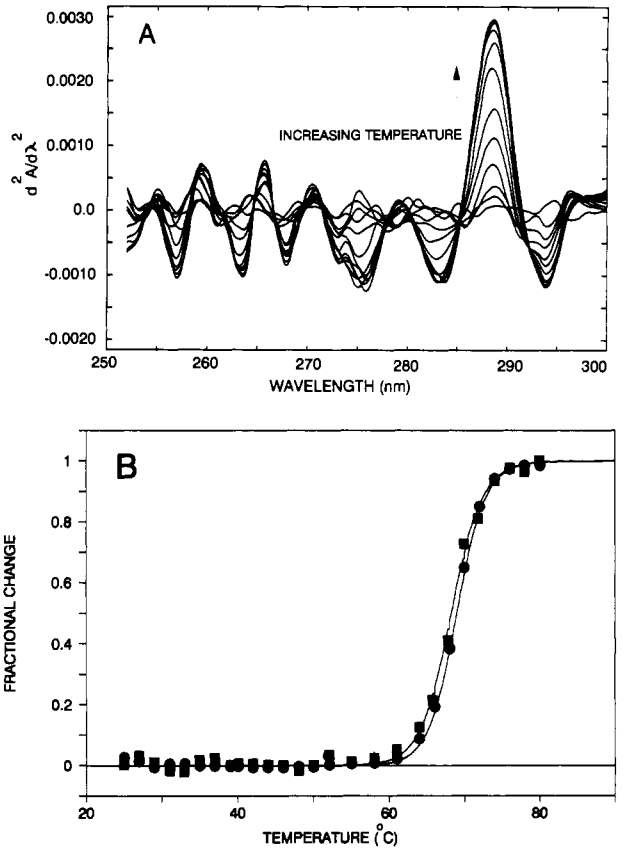

FIGURE 4: Thermally induced second-derivative difference spectra in the UV region for ferricytochrome b_{562}. These spectra were obtained by subtracting the observed second-derivative spectrum at the temperature of measurement from the initial (25 °C) spectrum. The cytochrome concentration used for this experiment was 30 μM. Thermally induced solvation changes surrounding the tyrosine residue(s) were monitored by an increased blue shift and increased absorbance change at 287 nm. (B) The van't Hoff fits of the temperature-dependent fractional changes due to heme absorption changes ($A_{530} - A_{800}$) (●) and tyrosine solvation (■) are coincident.

Discussion

The thermal denaturation profiles of ferri- and ferrocytochrome b_{562} follow a two-state transition as evidenced by excellent fits to a van't Hoff treatment of the temperature-dependent heme transitions and tyrosine solvation changes. The rate of equilibration between the native (N) and denatured (D) species appears to be fast, based on the independence of the thermodynamic parameters and the rate of temperature increase (Table II). Partial to nearly complete reversibility of the thermal denaturation equilibrium for this cytochrome is dependent on the time the denatured protein is kept above T_m. This suggests that other forms of the denatured cytochrome can exist in addition to the initial thermally denatured form, D (see Results). For the ferricytochrome form, changes in the temperature-dependent heme transitions are coincident with denaturation profiles due to increases in tyrosine solvation. This observation further supports the contention that the thermal denaturation of this protein can be adequately modeled as a two-state transition.

Preliminary thermal denaturation experiments using ferricytochrome b_{562} were performed by Myer and Bullock (1978). A comparison of the results obtained by these investigators with the results presented here reveals both similarities and differences. Specifically, the T_m value (67 °C) for thermal denaturation reported by Myer and Bullock agrees

with the value obtained in the present study (66.7 °C). More importantly, these investigators also observed a loss of α-helical secondary structure during the thermal unfolding process centered at 67 °C as indicated by the loss of absorbance at 220 nm monitored by circular dichroism spectroscopy. Thus, thermal changes in heme and aromatic amino acid absorbances coincide with the loss of secondary as well as tertiary structure of the protein. However, Myer and Bullock propose that the thermal denaturation for this cytochrome occurs in two distinct steps. These two transitions are centered at 35 and 67 °C with corresponding enthalpies of 23 and 75 kcal/mol, respectively. On the basis of circular dichroism measurements, these investigators conclude that the first transition reflects the unfolding or relaxation of the heme environment. Examination of the thermally induced changes (25–50 °C) in solvation of aromatic residues located in the heme binding site, monitored by second-derivative analysis and absorbance changes attributed to the heme moiety, show gradual changes in absorbance with no evidence for an earlier transition. The pretransition changes in tyrosine solvation and heme absorption exhibit excellent linear fits as evidenced by the flat base lines (Figures 3 and 4). This observation indicates that these changes simply represent a gradual temperature-dependent change in extinction coefficients. The reasons for the discrepancy between the thermal transition data of Myer and Bullock (1978) and those presented in this paper are not known. It is probable that thermally induced changes in the asymmetric environments of both the heme moiety and the aromatic residues monitored by circular dichroism spectroscopy would be spectrally silent in the measurements used in this study. Recently, Wu et al. (1991) have found that the heme of cytochrome b_{562} exhibits asymmetric heme contact shifts patterns by ^{1}H NMR which they attribute to heme orientation disorder. These investigators also have evidence for the existence of a spin equilibrium for an intact His/Met ligation for cytochrome b_{562}. Changes in the electron distribution and the heterogeneity in heme orientation could be the source of the temperature-dependent CD changes observed by Myer and Bullock (1978). The presence or absence of this transition does not affect the interpretation of the thermal unfolding results presented here.

The most significant result from the present thermal denaturation studies is the observation that the thermal stability of cytochrome b_{562} is dramatically enhanced following the one-electron reduction of the protein-bound heme iron. The difference in Gibbs energy for thermal unfolding of ferri- an ferrocytochrome b_{562} at the ferricytochrome T_m, $\Delta\Delta G$, can be obtained by using the relationship $\Delta\Delta G = \Delta T_m \Delta S_m$, where ΔT_m is the T_m difference between the ferri- and ferrocytochrome and ΔS_m is the entropy change for the ferricytochrome (Becktel & Schellman, 1987). Given the above equation, when ΔT_m = 14.3 °C and ΔS_m = 324 cal/(K·mol), then $\Delta\Delta G$ = 4.6 kcal/mol, which represents a substantial increase in thermal stability. In addition to the increased overall stability, the Gdn-HCl-induced rate of heme dissociation for the oxidized form is 4 orders of magnitude faster than the rate observed for the reduced form. This drastic difference in heme dissociation rates indicates that the reduced heme binds more tightly to the protein than does the oxidized heme.

The measurement of thermal stability differences inherently represents a "low resolution" technique for detecting structural differences between two conformers of a protein. More definitive information regarding the extent of structural changes often requires additional experimental information to narrow the possible molecular sources of thermal stability differences. Using NMR spectroscopy, Moore and co-workers (Moore et al., 1985) observed that a heme meso resonance was not exchange-broadened during a redox titration of cytochrome b_{562}. From the chemical shift difference of this resonance (3.3 ppm), the calculated electron self-exchange rate for this cytochrome is fast (4×10^6 M^{-1} s^{-1} at 42 °C, pH 7.0). On the basis of this observation, they conclude that the conformational changes accompanying a change in the redox state of this cytochrome are small. Thus, it can be inferred that the nuclear reorganizational energy accompanying an electron-transfer reaction for cytochrome b_{562} is also small. This is consistent with the idea that small, soluble electron-transfer proteins which function as shuttles between different donor and acceptor electron-transfer proteins would exhibit minimal structural alterations following a change in redox state (Gray & Malmström, 1989).

Important new insights concerning the origin of redox-linked conformational changes in small electron-transfer proteins are beginning to emerge. Recently, Englander and co-workers (Feng et al., 1990) have utilized main-chain NMR assignments in cytochrome c to determine whether the redox-dependence chemical shifts reflect large structural changes. Their results suggest that the various physicochemical differences observed between the oxidized and reduced conformers reflect changes in structural dynamics rather than large changes in the three-dimensional structure. They conclude that the source of the physical–chemical differences frequently observed between redox states in heme proteins is due to increased binding of the reduced heme to the protein. The dramatic difference in the observed Gdn-HCl-induced heme dissociation rates presented here supports this conclusion.

At the molecular level, the dynamics or overall flexibility of redox proteins could be the result of redox-linked strain manifested through increased bonding strengths of the axial ligands to the reduced heme and through Coulombic interactions between the redox center and surface residues. Both of these molecular aspects will contribute to the observed thermal stability. The generation of a partially buried positive charge arising from the protein-bound ferric heme–iron during oxidation may enhance (1) repulsive interactions between surface charges and (2) ionizations of surface amino acid side chains. Increased ionizations could lead to further repulsion and, hence, increase the separation and flexibility of surface secondary elements (Trewhella et al., 1988; Lui et al., 1989).

Since proper orientation and specificity between redox centers in proteins is initially dictated by electrostatic interactions (Matthew et al., 1983), subtle changes in surface charge between redox states of an electron-transfer protein is, perhaps, a major determinate of biological specificity for electron-transfer reactions. Small changes in the pK_a of individual charged residues might affect the lifetime of the protein–protein electron-transfer complexes prior to electron-transfer events. Recently, Englander and co-workers have observed selective phosphate binding at a lysine-rich site localized on the surface of oxidized cytochrome c (Feng & Englander, 1990). Subtle changes in surface change indicated by these data might explain why ferri- and ferrocytochrome c exhibited different elution profiles from cation-exchange columns (Margolish, 1954). For cytochrome b_{562} five redox-dependent proton ionizations have been observed thus far. Two of these ionizations occur in the ferrocytochrome form (Moore et al., 1985). Future studies aimed at identifying which residues in cytochrome b_{562} undergo redox-linked ionizations and quantifying their effects on the structural dynamics, thermostability, and reduction potentials will contribute important information for elucidating the functional

and structural consequences of simple one-electron reductions in small, globular electron-transfer proteins.

ACKNOWLEDGMENTS

I thank Drs. H. Nikkila and S. G. Sligar for their generous donation of purified cytochrome b_{562}.

REFERENCES

Bechtold, R., Kuehn, C., Lepre, C., & Isied, S. (1986) *Nature (London) 322*, 286–288.

Becktel, W. J., & Schellman, J. A. (1987) *Biopolymers 26*, 1859–1877.

Demchenko, A. P. (1986) *Ultraviolet Spectroscopy*, p 123, Springer-Verlag, Berlin.

Dokter, P., van Wielink, J. E., van Kleef, M. A. G., & Duine, J. A. (1988) *Biochem. J. 254*, 131–138.

Eden, D., Matthew, J. B., Rosa, J. J., & Richards, F. M. (1982) *Proc. Natl. Acad. Sci. U.S.A. 79*, 815–819.

Edge, V., Allwell, N. M., & Sturtevant, J. M. (1985) *Biochemistry 24*, 5866–5906.

Englander, S. W., Calhoun, D. B., & Englander, J. J. (1987) *Anal. Biochem. 161*, 300–306.

Feng, Y., & Englander, S. W. (1990) *Biochemistry 29*, 3505–3509.

Feng, Y., Roder, H., & Englander, S. W. (1990) *Biochemistry 29*, 3494–3504.

Gray, H. B., & Malmström B. G. (1989) *Biochemistry 28*, 7499–7505.

Guggenheim, E. A. (1926) *Philos. Mag. 2*, 538.

Hoffman, B. M., & Ratner, M. A. (1987) *J. Am. Chem. Soc. 109*, 6237–6243.

Hu, C. Q., & Sturtevant, J. M. (1987) *Biochemistry 26*, 178–182.

Ichikawa, T., & Terada, H. (1979) *Biochem. Biophys. Acta 671*, 33–37.

Itagati, E., & Hager, L. P. (1966) *J. Biol. Chem. 241*, 3695–3700.

Kharakoz, D. P., & Mkhitaryan, A. G. (1986) *Mol. Biol. (Eng. Transl.) 20*, 312.

Liu, G., Grygon, C. A., & Spiro, T. G. (1989) *Biochemistry 28*, 5046–5050.

Manly, S. P., Matthews, K. S., & Sturtevant, J. M. (1985) *Biochemistry 24*, 3842–3846.

Marcus, R. A., & Sutin, N. (1985) *Biochim. Biophys. Acta 811*, 265–322.

Margolish, E. (1954) *Biochem. J. 56*, 535–539.

Mathews, F. S., Bethge, P. H., & Czerwinski, E. W. (1979) *J. Biol. Chem. 254*, 1699–1709.

Matthew, J. B., Weber, P. C., Salemme, F. R., & Richards, F. M. (1983) *Nature (London) 301*, 169–171.

McLendon, G., Pardue, K., & Bak, P. (1987) *J. Am. Chem. Soc. 109*, 7540–7541.

Moore, G. R., Williams, R. J. P., Peterson, J., Thomson, A. J., & Mathews, F. S. (1985) *Biochim. Biophys. Acta 829*, 83–96.

Myer, Y. P., & Bullock, P. A. (1978) *Biochemistry 17*, 3723–3729.

Nikkila, H. (1987) Ph.D. Thesis, University of Illinois, Urbana.

Trewhella, J., Carlson, V. A. P., Curtis, E. H., & Heidorn, D. B. (1988) *Biochemistry 27*, 1121–1125.

Ulmer, D. D., & Kagi, J. H. R. (1968) *Biochemistry 7*, 2710–2723.

Wu, J., La Mar, G. N., Yu, L. P., Lee, K.-B., Walker, F. A., Chiu, M. L., & Sligar, S. G. (1991) *Biochemistry 30*, 2156–2165.